УДК 519.9

Мегреганіан Н.[1], канд. наук,
Фаллах А.С.[2], канд. наук
Люка Л.А.[1], канд. наук

## Великі пружно-пластичні деформації квадратних мембран під дією локалізованих імпульсних навантажень

[1] Imperial College London, London, Exhibition Road, London SW7 2AZ UK
e-mail: n.mehreganian14@imperial.ac.uk
[2] Brunel University, Kingston Lane, London, Uxbridge, UB8 3PH UK
e-mail: mestasf@brunel.ac.uk

N. Mehreganian[1], Ph.D.
A.S. Fallah[2], Ph.D.
L.A. Louca[1], Ph.D.

## Large elastic-plastic deformation of square membranes subjected to localised pulse pressure loads

[1] Imperial College London, London, Exhibition Road, London SW7 2AZ UK
e-mail: n.mehreganian14@imperial.ac.uk
[2] Brunel University, Kingston Lane, London, Uxbridge, UB8 3PH UK
e-mail: mestasf@brunel.ac.uk

*Дана робота зосереджена на пружній і еластичній енергіях мембрани і має ціллю виведення, шляхом мінімізації енергетичного функціоналу в поєднанні з визначальними співвідношеннями скінченого аналізу, динамічного пружно-пластичного відгуку квадратних мембран на локалізоване ударне навантаження, що приводить до великих деформацій. Припускається, що функція вибухового навантаження має вигляд мультиплікативного розкладу заданої безперервної кусково-гладкої просторової функції та довільної функції часу, яка може приймати різні часові форми.*

*Ключові слова: ударне навантаження, квадратна мембрана, метод Рітца-Гальоркіна.*

*Ductile isotropic materials are widely used in protective systems against transient pulse pressure loads, such as those of localised blasts. This is due to the combined elastic-plastic response which contributes to dissipation of total impulse from extensive loading as the energy stored elastically limits deformation while the energy expended plastically limits the level of transferred forces in the structure. In the case of thin, modern armour graded steel plates, the tailored metallurgy helps the structure store energy within the bounds of elastic region, which may be dissipated at a later stage as damping kills it off in subsequent cycles. On the other hand, the plastic work is almost entirely converted to heat and dissipates.*

*The present work focuses on the elastic and plastic energies in the membrane and aims at deducing, from the minimization of Föppl-Von-Kármán (FVK) energy functional combined with enforcing the constitutive relations of limit analysis, the dynamic elastic-plastic response of localised blast loaded square membranes undergoing large deformations. The presumed blast load function is a multiplicative decomposition of a prescribed continuous piecewise smooth spatial function and an arbitrary temporal function which may assume various temporal shapes (e.g. rectangular, linear, exponential).*

*Considering the elastic response, a single-degree-of-freedom model was developed from the prescribed displacement field and associated stress tensor having clamped and simply supported boundary conditions. The explicit closed form solutions were sought by using the Ritz-Galerkin's variational method as well as the Poincaré-Lindstedt perturbation method. The theoretical solutions of rigid-perfectly plastic square membranes subjected to the same blast scenarios were then discussed. From the combined effects we deduce the load displacement curves representing the trajectory of the nonlinear elastic-perfectly plastic structure.*

*Key Words: localised blast, square membrane, Ritz-Galerkin method.*

Статтю представив д. ф.-м. н., проф. Жук Я.О.

### 1. Introduction

Transient pulse pressure loads, such as those from gas or IED (Improvised Explosive Device) explosions, generate high velocity impulse ensuing the large deformations and potential failure of the structural components. The level of damage depends on the source of impulse, the stand-off distance, high explosive mass geometric configurations.

Most protective structural systems, such as blast walls, shutters, doors, as well as armored vehicles

components, are designed in the form of plated elements. These elements can be fabricated from ductile isotropic materials such as modern armour graded steel with high load bearing capacity beyond the initial yield point, leading to an elastic-plastic response. Such alloys possess high yield strength and low ductility, whereby the elastic strain energy becomes significant.

Assuming the load duration is insignificant compared to the structural component's natural period of vibration while the component is made of strain rate insensitive material and no hardening, the visco-elasticity and visco-plasticity phenomena can be ignored, the constitutive tensor may be treated as that of elastic-perfectly plastic material. The elastic analysis provides a useful insight into predicting the complex response of quasi-brittle, thin structural plated elements, such as glass panes, composites and thin armour steel plates. The latter is a suitable candidate material for blast protection as it bears high elastic energy capacity preceding its small plastic deformation [1], [2].

The present study deals with applying the well-established Föppl-Von-Kármán model to address the influence of finite displacement, or geometry changes in the overall response of the structure, in light of the developed membrane resistance in conjunction with the bending resistance of the structure. The objective of this work is to examine the explicit solutions delineating geometric and material nonlinearity of ductile, isotropic homogeneous square plates to the transient blast pressure with generic spatial function as described in Eq.(1). The plates investigated herein are assumed as thin, where the terms of transverse shear from the Mindlin-Reisner plate theory can be neglected, but as the external force maps the material coordinates in reference configuration to the deformed state, the response of the structure is characterised by the deformed configuration, rather than the reference configuration. Thus, the influence of finite displacements, or geometry changes, due to the presence of membranal forces must be retained in the analysis performed. This is achieved by implementing the well-known Föppl-Von-Kármán (FVK) nonlinear theory together with the constitutive framework of limit analysis.

The current work is organized in four sections and entails a description of the localised blast in section 1, followed by the derivation of the governing equations of membrane elasticity in section 2. In Section 3, the theoretical solutions at two distinct phases of motion are investigated, followed by the elastic-plastic response of the membrane elements. Finally, the concluding remarks are presented in section 4.

### 1.1 Localised Pulse Pressure Load

Consider an initially flat, monolithic, ductile isotropic square plate with side length $2L$, thickness of $H$ and areal density of $\mu = \rho H$. The plate is secured along its periphery with simply supported boundary conditions and subjected to a localised pressure load. Such a load may be truncated into a single term of multiplicative decomposition of its temporal (pulse shape) and spatial (load shape) functions [1], [3]–[6], as presented in Eqs. (1)-(2). As the load is axisymmetric the domain of study is reduced to only one quarter of the plate.

$$p_1(r) = \begin{cases} p_0, & 0 \le r \le R_e, \\ p_0 a\, e^{-br}, & R_e \le r \le R \end{cases} \tag{1}$$

$$p_2(t) = \begin{cases} 1, & 0 \le t \le t_d, \\ 0, & t \ge t_d \end{cases}. \tag{2}$$

Using the Ritz-Galerkin's method, load functional is minimised in Eq.(3). The load is rotationally symmetric, thus independent of the polar coordinate $\theta$. It follows that, with $x = r\cos\theta$ and $y = r\sin\theta$, the functional of Eq.(3) may be furnished into a single dimensionless parameter $\alpha$ in Eq.(4), which is influenced by the central constant load radius $R_e$ as well as the load decay exponent $b$:

$$\int_0^{\frac{\pi}{2}}\int_0^{R_e} p_0 \delta w\, r\, dr\, d\theta + \int_0^{\frac{\pi}{2}}\int_{R_e}^{L} p_0\, e^{-(br-bR_e)} \delta w\, r\, dr\, d\theta = \alpha p_0 L^2 \tag{3}$$

where $\delta w = \cos\left(\frac{\pi x}{2L}\right)\cos\left(\frac{\pi y}{2L}\right)$,

$$\alpha = \frac{32}{\pi\left(4L^2b^2+\pi^2\right)^2}\left[\left(\frac{1}{16}\pi^4 bR_e + \frac{1}{4}L^2b^2(bR_e+3)\pi^2 + L^4b^4\right)\cos\frac{\pi R_e}{2L} + \frac{1}{8}\pi^3\left(b^2L^2 + 2Lb + \frac{1}{4}\pi^2\right)e^{-b(L-R_e)} - \left(b^2L^2+\frac{1}{4}\pi^2\right)^2\right].$$

It is straightforward to show that the various values of $\alpha$ converge to a unique parameter pertinent to the case of uniformly distributed load as $R_e \to L$, independent of the decay type.

### 2. Governing Equations

The FVK Equations describing the fundamental description of nonlinear elastic dynamics of the thin plate reads[7]:

$$D\nabla^4 w(x,y,t) - H\ell(w,\Phi) = p(x,y,t)\,, \quad (5)$$

$$\nabla^4\Phi(x,y,t) = -\frac{E}{2}\ell(w,w) \Leftrightarrow -E\left(\kappa_x\kappa_y - \kappa_{xy}^2\right) \quad (6)$$

It is assumed that the reference configuration is stress free and the material elements and behave isotopically relative to the reference configuration. The right-hand side of Eq.(6) represents Gaussian curvature which is quadratic with respect to the transverse displacement field, while the term $\Phi(x,y,t)$ denotes the Airy stress function. This function describes the membrane action induced by large displacements. In Eq.(5) $D = \frac{EH^3}{12\left(1-\nu^2\right)}$ is the flexural rigidity of the plate, while the biharmonic operator $\nabla^4$ and the differential operator $\ell(w,\Phi)$ are expressed in Eqs.(7) and (8), respectively.

$$\nabla^4\Phi = \frac{\partial^4\Phi}{\partial x^4} + 2\frac{\partial^4\Phi}{\partial x^2\partial y^2} + \frac{\partial^4\Phi}{\partial y^4}\,, \quad (7)$$

$$\ell(w,\Phi) = \frac{\partial^2 w}{\partial^2 x}\frac{\partial^2\Phi}{\partial^2 y} + \frac{\partial^2 w}{\partial^2 y}\frac{\partial^2\Phi}{\partial^2 x} - 2\frac{\partial^2 w}{\partial y\partial x}\frac{\partial^2\Phi}{\partial x\partial y} \quad (8)$$

Hence the term $\ell(w,w)$ from the compatibility Eq.(6), is evaluated by replacing $\Phi$ with $w$ in Eq.(9). Eqs. (5)-(8) are coupled, highly nonlinear, fourth order Partial Differential Equations (PDE) which represent geometric nonlinearities of an elastic system induced by in-plane displacements and membranal forces.

The approach resorted to herein to solve the FVK equations seeks, by utilizing an iterative procedure, to reduce the PDE to an Ordinary Differential Equations (ODE) using the Poincaré-Lindstedt (P-L) perturbation technique, combined with the RG method. The mathematical procedure for such shell elements is outlined as follows:

1. Assume an ansatz for displacement fields and the associated stress tensors.
2. Determine the membranal stress from the compatibility relation of Eq. (9).
3. Update the displacement field from Eq.(5).
4. The final form of transverse displacement will be nonlinear, but in a reduced closed form expression.

The assumed expressions of the displacement field and the associated Airy stress functions may be expressed as multiplicative decomposition into a spatial part as well as that of the temporal part, i.e.

$$w(x,y,t) = H\overline{w}(t)\,w^*(x,y) \quad (9)$$

$$\Phi(x,y,t) = f(t)\,\phi^*(x,y) \quad (10)$$

where the prescribed partial functions $w^*(x,y) = \phi^*(x,y)$ is assumed as the first term of the trigonometric truncation $\cos\left(\frac{n\pi x}{2L}\right)\cos\left(\frac{m\pi y}{2L}\right)$, which characterises the vibration of a Single Degree of Freedom model, i.e., they are associated with the first (fundamental) mode of vibration. Accordingly, the dimensionless parameters $\bar{\phi} = \frac{f(t)}{EH^2}$, and $\overline{w}(t) = \frac{w(0,0,t)}{H}$ have been employed.

The RG variational technique to minimize the total elastic energy functional can be sketched in Eqs.(11a-b), where the superscript (i) denotes the iteration. With this strategy, as discussed earlier, we may dynamically update the interrelation between the transverse displacement field in Eq. (11a) from the state of membranal stress tensors satisfying Eq.(11b) , and vice versa.

### 3. Dynamic Response

#### 3.1 First Phase of Motion (Forced Vibration)

Substituting Eqs.(9) and (10) in Eqs. (11, a-b) and performing the integrations reduces the FVK Partial Differential Equation to an ODE in the form of (12)

$$\iint_{(A)}\left\{D\nabla^4\overline{w}^{(i+1)} - H^3E\,\ell\left(\overline{\mathbf{w}}^{(i)},\overline{\mathbf{\Phi}}^{(i+1)}\right) + {}^{(..)}\mu\overline{w}^{(i+1)}\right\}\delta w\,dA = \iint_{(A)}\frac{p(x,y,t)}{H}\delta w\,dA \quad (11a)$$

$$\iint_{(A)}\left\{\nabla^4\overline{\Phi}^{(i+1)} + \frac{1}{2}\ell\left(\overline{w}^{(i)},\overline{w}^{(i)}\right)\right\}\delta\Phi\,dA = 0 \quad (11b)$$

$$\omega_e^2 \overline{w}^{(i+1)} + {}^{(..)}w^{(i+1)} - \frac{3E\pi^2\varepsilon}{4\rho L^2}\overline{w}^{(i)}\overline{\phi}^{(i+1)} = \frac{4\alpha p_0}{\rho H^2} \quad (12)$$

where $\varepsilon = \frac{8H^2}{9L^2}$ is a parameter of small value. From the compatibility equation (11-b) we obtain:

$$\overline{\phi}^{(i+1)} = -\frac{4}{3\pi^2}\overline{w}^{(i)^2} \quad (13)$$

The coefficient of the nonlinear term $\overline{w}^{(i)}\overline{\phi}^{(i+1)}$, may be visualized as the equivalent membrane stiffness of the plate; for a multiple degree of freedom system, this nonlinear term accounts for the mode coupling of the structure. The vibration frequency $\omega_e^2$ gives the ratio of the bending stiffness to the equivalent mass of the structure expressed as:

$$\omega_e = \frac{1}{2}\frac{\pi^2}{L^2}\sqrt{\frac{D}{\mu}} \quad (14)$$

The solution to the first iteration $\overline{w}^{(1)}$ is derived by linearizing the form of the ODE in Eq.(12), i.e. eliminating the Airy Stress function terms $\overline{\phi}^{(i+1)}$. The general solution to the plate motion must satisfy the initial kinematic conditions $\overline{w}(0) = \dot{\overline{w}}(0) = 0$, and can be sketched as:

$$\overline{w}^{(1)} = c(1 - \cos\omega_e t) \quad (15)$$

where the amplitude of vibration is

$$c = \frac{4\alpha p_0}{\rho H^2 \omega_e^2}. \quad (16)$$

While the expression of the transverse displacement in further iterations may be derived by substituting Eq. (15) in Eq. (13) and then in Eq. (11a), heuristically, with the nonlinear terms present in Eq.(12), the explicit solution entails the presence of secular terms (in the form of $t\sin t$) which brings about a non-harmonic response with unbounded growth of transient displacements. The solution can be made harmonic by employing the Poincaré-Lindstedt perturbation method to eliminate, once and for all, the dependence of the displacement field on such terms. To this end, the frequency response is normalised as $\tau = \left(\omega_e + \varepsilon\overline{\omega}_i + O(\varepsilon^2)\right)$, where $\overline{\omega}_i$ is referred to as the pseudo vibration hereinafter at the phase (i)$^{th}$ of motion. Accordingly, the displacement field is expressed as a truncated series of its iterative terms given by:

$$\overline{w}(\tau) = \overline{w}^{(1)}(\tau) + \varepsilon\overline{w}_1^{(2)}(\tau) + O(\varepsilon^2) \quad (17)$$

$$\tau = \left(\omega_e + \varepsilon\overline{\omega}_1 + O(\varepsilon^2)\right)t \quad (18)$$

To derive the ODE expression for the second term, we shall hence forth ignore the terms of higher order as $\varepsilon^2 << 1$. Hence, substituting Eq. (17) and (18) in Eq. (12) together with the use of Eq. (15) yields

$$\omega_1^2\left(\overline{w}^{(2)} + {}^{(..)}\overline{w}^{(2)}\right) + 2\omega_e{}^{(..)}\overline{\omega}_1^{(1)}c\overline{w} + \frac{E\varepsilon}{\rho L^2}\left(\overline{w}^{(1)}\right)^3 = 0 \quad (19)$$

Sequentially, the ODE of Eq.(19) is re-evaluated and solved to determine, unequivocally by imposing the initial boundary conditions, the plate maximum transverse displacement as

$$\overline{w}^{(2)} = -\frac{c\tau\sin\tau}{8\omega_e^2 L^2\rho}\left(8L^2\omega_e\overline{\omega}_1\rho - 15Ec^2\right) + C_2\sin\tau + C_1\cos\tau - c/\left(8\omega_e^2 L^2\rho\left(Ec^2\left(\cos\tau^3 - 8\cos\tau^2 - 15\cos\tau + +24\right) + 8L^2\cos\tau\,\omega_e\,\omega_1\,\rho\right)\right), \quad (20)$$

where the integration constants are

$$C_2 = 0, \quad C_1 = \left(17c^3E\right)/\left(8\omega_e^2L^2\rho\right) \quad (21)$$

While the expression of pseudo vibration term to eliminate the secular term is given as

$$\overline{\omega}_1 = \frac{15Ec^2}{8L^2\omega_e\rho}, \quad (22)$$

which recasts Eq.(20) into Eq. (23). The dependence of this parameter on the plate slenderness ratio and load parameters is illustrated in Fig 1.

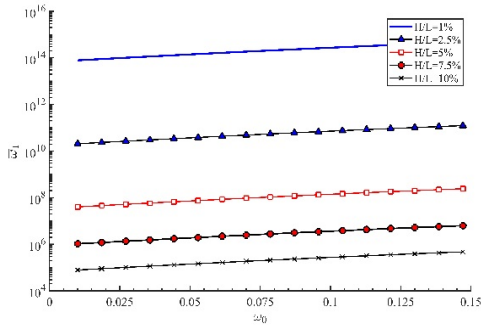


Fig. 1- Variations of the pseudo vibration with central uniform load radius (with $b = 50m^{-1}$)

$$\overline{w}^{(2)} = -\frac{Ec^3}{8\omega_e^2 L^2 \rho}\left(\cos\tau - 1\right)\left(\cos\tau^2 - 7\cos\tau - 24\right) \quad (23)$$

### 3.2 Second Phase of Motion (Free Vibration)

The loading is complete at time $t = t_d$; however, the system retains its motion due to the initial inertia effects and the energy stored in it. It follows that the associated response of the plate is governed by a free vibration following the forced vibration of the previous phase. Subsequently, at the time point of completion of loading, the kinematic continuity applies to ensure there is no displacement or velocity jumps throughout the motion.

The analysis in this phase is carried out in the same spirit as the previous phase of motion- with the solution of linear and nonlinear parts of the displacement field determined on $\overline{\phi}^{(1)} = 0$ (or $\varepsilon \downarrow 0 = 0$), and on $\overline{\phi}^{(2)}$ respectively. Provided that the nonlinear terms are disregarded, the first iteration of ODE is expressed, using the kinematic continuity of displacement and velocity fields of each mode at $t = t_d$, as:

$$\overline{w}^{(1)} = c\left(\cos\omega_e\left(t - t_d\right) - \cos\omega_e t\right) \quad (24)$$

The plate reaches its peak transient deformations when the velocity vanishes, i.e. $\dot{\overline{w}}^{(i)} = 0$, occurring at

$$t_{\max} = \frac{1}{2\omega_e}\left(\left(2k-1\right)\pi + \omega_e t_d\right), \quad (25)$$

where $k$ is an integer. A plot of the maximum transient deformation against various load magnitudes is illustrated in Fig. 2.

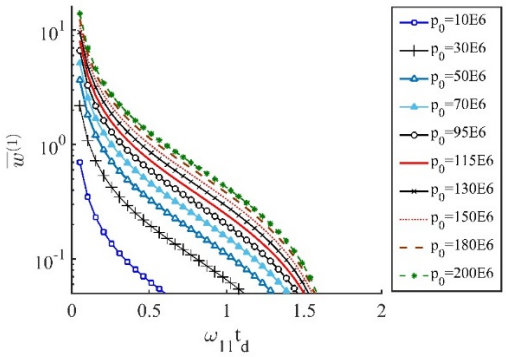


Fig. 2- Variations of the peak transient Mid-point deflection with load magnitude

In the same spirit, Eq. (24) was employed to evaluate the solutions of the ODE (19) as:

$$\overline{w}^{(2)} = C_3\sin\tau + C_4\cos\tau + \frac{Ec^3}{32L^2\omega_e^2\rho}\left(\cos\left(3\tau - 3\tau_1\right) - \right.$$
$$\left. - 3\cos\left(3\tau - 2\tau_1\right) + 3\cos\left(3\tau - \tau_1\right) + \right.$$
$$\left(\frac{16L^2\omega_e\overline{\omega}_2\rho}{Ec^2} - 18\right)\left(\cos\left(\tau - \tau_1\right) - \cos\tau\right) +$$
$$\left. + 6\cos\left(\tau - 2\tau_1\right) - 6\cos\left(\tau - \tau_1\right) - \cos\ldots..\right) . \quad (26)$$

In expression (26) the condition to make the response harmonic is imposed by, using algebraic manipulations, deriving the solution of the parameter $\overline{\omega}_2$, as expressed in Eq. (27), to eliminate the secular term. It turns out that the pseudo vibration in this phase is pulse dependent, while a surface plot of its variation with the load parameters is drawn in Fig 3. The integration constants were attained by imposing the kinematic continuity, given in Eqs. (28 a-b).

$$\overline{\omega}_2 = \frac{3}{4}c^2 E\frac{\left(1-\cos\tau_1\right)}{\rho L^2\omega_e} \quad (27)$$

$$c_3 = \frac{Ec^3}{16\omega_e^2 L^2\rho}\sin\tau_1\left(2\cos\tau_1^3 + 6\cos\tau_1^2\sin\tau_1 - 26\cos\tau_1^2 - \right.$$
$$\left. - 32\cos\tau_1\sin\tau_1 - 37\cos\tau_1 - 34\sin\tau_1 + 1\right) \quad (28a)$$

$$c_4 = \frac{1}{8}\frac{Ec^3}{16\omega_e^2 L^2\rho}\left(\frac{37}{2} + \cos\tau_1^4 + \left(3\sin\tau_1 - 13\right)\cos\tau_1^3 - \right.$$
$$\left. - \left(16\sin\tau_1 + \frac{37}{2}\right)\cos\tau_1^2 + \left(-17\sin\tau_1 + 12\right)\cos\tau_1\right) \quad (28b)$$

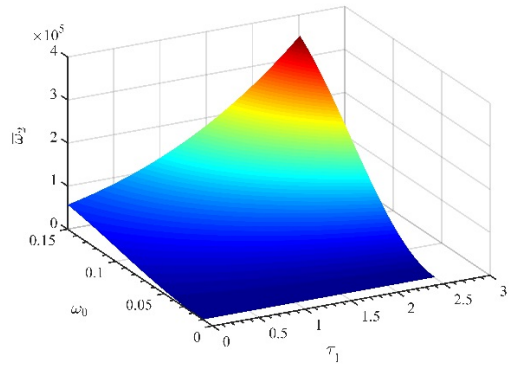


Fig. 3 Variations of the pseudo vibration $\overline{\omega}_2$ with central uniform load radius (with $b = 50m^{-1}$)

### 3.3 Elastic-Plastic response of the plates

As an extensive transient load is imparted on the structure, the plastic hinges may form in local boundary elements and/or the central zones while the remaining of the plate would behave elastically. The regions where plastic flow occurs may appear intermittently. It turns out that finding the plastic deformation can be difficult as they are inter-spread with elastic deformations. In the past, however, the actual response of the structure has been simplified

into a three stage of elastic-plastic response: the first stage presumed as wholly elastic, which terminates when the yield criterion is invoked, followed by a rigid, perfectly plastic stage. Finally, the motion is concluded with a residual elastic vibration, corresponding to a 'latent' elastic strain energy of the rigid-plastic stage [8]–[11]. The three-stage analysis may be idealised, preferably, into a primarily dominating rigid-plastic form solution with infinite elastic stiffness, together with the 'latent' elastic deformations by permitting the flexural rigidity to revert to its actual value from infinity. The actual deformations would be summation of the rigid-plastic part as well as the elastic deformations.

However, this simplification remains valid provided the material obeys the Hook's law (linear elastic response) during the elastic vibrations, which may not be pertinent to the case of extensive blast loads inducing geometric nonlinearities in the plate. Furthermore, most materials exhibit such nonlinearities in the elastic state with some/little plasticity. Thus, it is pragmatic to investigate the elastic-plastic response of the plated elements where the influence of the membrane forces plays a significant role throughout the structural response.

The foregoing analysis assumed the material performance is wholly elastic. Indeed, the material points through plate section strain plastically when the trajectory of the stress state reaches the yield curve of the associated constitutive yield criterion. Since large nonlinear deformations are of concern, it may be presumed that the bending strain energy is insignificant to the membrane strain energy. To determine the elastic-plastic deformations, it is assumed that the response is predominantly governed by the membrane forces.

Evaluating the components of the Cauchy stress tensor from the Airy stress function, we have:

$$\sigma_x = \frac{\partial^2 \Phi}{\partial y^2}, \quad \sigma_y = \frac{\partial^2 \Phi}{\partial x^2}, \quad \sigma_{12} = \frac{\partial^2 \Phi}{\partial y \partial x}, \qquad (29)$$

where $\sigma_{12}$ represents the shear stress. In 2-dimensional state of stress, the principle stresses represent the eigenvalues of the Cauchy stress tensor as

$$\sigma_k = \frac{\sigma_x + \sigma_y}{2} \pm \left[ \left( \frac{\sigma_y - \sigma_x}{2} \right)^2 + \sigma_{12}^2 \right] \qquad (30)$$

with $k = 1,2$ giving the maximum and minima of the principle stresses, respectively. Eqs. (29) is utilised, together with Eq.(30), to delineate the membrane forces in principle directions is evaluated as (34)-(35):

$$N = \int \sigma_k dZ , \qquad (34a)$$

$$N = -\frac{1}{4L^2} \pi^2 \bar{\phi}^{(i+1)} H \cos \frac{\pi (x+y)}{2L} \qquad (34b)$$

From Eq. (34), the membrane plastic collapse capacity per unit length of the structure is given as:

$$N_0 = \sigma_0 H \qquad (35)$$

Equation (35) states a quadratic relationship of the transverse displacement field with the membranal forces, which attains a peak at each peak of displacement field. When $N = N_0$ the plate yields. Yielding occurs almost instantaneously before the plate reaches its first peak. The normalised membrane force displacement of armour steel and mild steel are plotted in Fig. 4 – Fig. 5 on four different square plates, namely, 4mm thick Mild steel, 4.61mm AR440T, 3.8mm AR370T and 4.16mm AR500T plates, the all having 400mm side length dimension. Details of the geometric and material properties of the candidates are found in [1]. The path of deformation, having reached the critical point of yielding, follows the straight line governed by Rigid-perfectly plastic theory. The permanent deformation of the plats may be found from the explicit solutions to rigid-perfectly plastic response of the plate in [6].

## 4. Concluding remarks

In this work we develop an analytical model to delineate the nonlinear dynamic response of elastic thin plated structures subject to transient pressure loads, such as localised blasts occurring due to proximal charges. The load was assumed to be multiplicatively decomposable into a spatial and a temporal distribution. Considering this idealization and utilising the Ritz-Galerkin's functional, a single dimensionless parameter was obtained which characterises various blast loading scenarios by the correct choice of its parameters $b, R_a$.

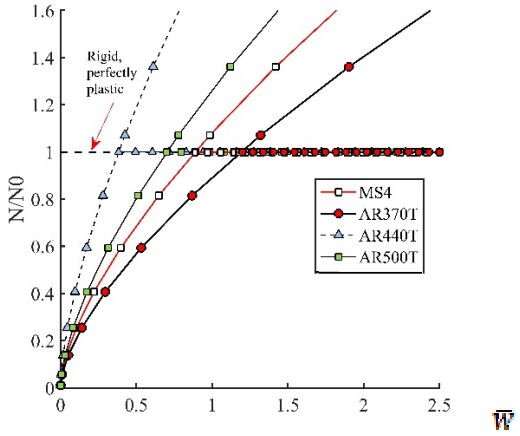


Fig. 4- Force vs normalised mid-point displacement of the panels subject to localised blast load with parameters $p_0 = 600\,MPa$ , $t_d = 20\mu s$ ,

$\frac{r_e}{L} = 0{,}33$; and $b = 50m^{-1}$

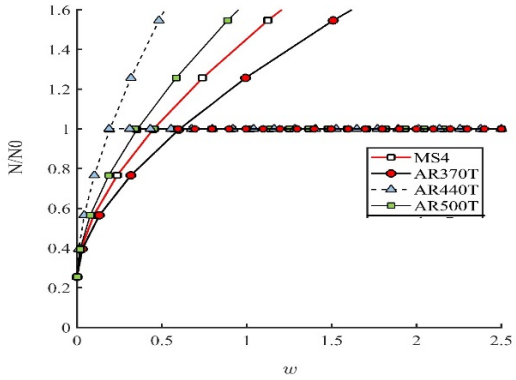


Fig. 5- Force vs normalised mid-point displacement of the panels subject to load parameters $p_0 = 20MPa$ , $t_d = 0{,}1\mu s$ and $\frac{r_e}{L} = 0{,}33$; and $b = 50m^{-1}$

The Ritz-Galerkin method was similarly employed, to minimize the nonlinear coupled FVK equations considering a kinematically admissible displacement field and an associated Airy stress function in an iterative procedure. The state variables were determined in two distinguished phases of motion, the first reflecting the forced vibration while the second addressing the free vibration due to initial inertia effects and the stored elastic energy of the system. The Poincaré-Lindstedt perturbation method was employed to avoid the non-convergent explicit solution due to the presence of secular terms whilst rendering the predicted oscillation harmonic.

The Elasto-plastic response of the plate was discussed by considering the plates as membrane, i.e., negligible bending stiffness compared with the membrane stiffness, with the assumption of perfect plasticity, i.e. neglecting the strain rate sensitivity and strain hardening phenomena.

## Список використаних джерел

1. Mehreganian, N. The response of mild steel and armour steel plates to localised air-blast loading-comparison of numerical modelling techniques / N. Mehreganian, L. A. Louca, G. S. Langdon, R. J. Curry, N. Abdul-Karim // Int. J. Impact Eng. – 2018. – **115**. – P. 81–93.

2. McDonald, B. Experimental response of high strength steels to localised blast loading / B. McDonald, H. Bornstein, G. S. Langdon, R. Curry, A. Daliri & A. C. Orifici // Int. J. Impact Eng. – 2017. – **115**. – P. 106–119.

3. Karagiozova, D. Simulation of the response of fibre-metal laminates to localised blast loading / D. Karagiozova, G. S. Langdon, G. N. Nurick & S. Chung Kim Yuen // Int. J. Impact Eng. – 2010. – **37(**6). – P. 766–782.

4. Fallah, A. S. Dynamic response of Dyneema® HB26 plates to localised blast loading / A. S. Fallah, K. Micallef, G. S. Langdon, W. C. Lee, P. T. Curtis & L. A. Louca // Int. J. Impact Eng. – 2014. – **73**. – P. 91–100.

5. Micallef, K. The dynamic performance of simply-supported rigid-plastic circular steel plates subjected to localised blast loading / K. Micallef, A. S. Fallah, D. J. Pope & L. A. Louca // Int. J. Mech. Sci. – 2012. – **65**(1). – P. 177–191.

6. Mehreganian, N. Inelastic dynamic response of square membranes subjected to localised blast loading / N. Mehreganian, A. S Fallah & L. A. Louca // Int. J. Mech. Sci. – 2018. – **148**. – P. 578–595.

## References

1. MEHREGANIAN, N., LOUCA, L. A., LANGDON, G. S., CURRY, R. J. & ABDUL-KARIM, N. (2018) The response of mild steel and armour steel plates to localised air-blast loading-comparison of numerical modelling techniques. *Int. J. Impact Eng.* 115. p. 81–93.

2. McDONALD, B., BORNSTEIN, H., LANGDON, G. S., CURRY, R., DALIRI, A., & ORIFICI, A. C. (2017) Experimental response of high strength steels to localised blast loading. *Int. J. Impact Eng.* 115. p. 106–119.

3. KARAGIOZOVA, D., LANGDON, G. S., NURICK, G. N. & CHUNG KIM YUEN, S. (2010) Simulation of the response of fibre-metal laminates to localised blast loading. *Int. J. Impact Eng.* 37 (6). p. 766–782.

4. FALLAH, A. S., MICALLEF, K., LANGDON, G. S., LEE, W. C., CURTIS, P. T. & LOUCA, L. A. (2014) Dynamic response of Dyneema® HB26 plates to localised blast loading. *Int. J. Impact Eng.* 73. p. 91–100.

5. MICALLEF, K., FALLAH, A. S., POPE, D. J. & LOUCA, L. A. (2012) The dynamic performance of simply-supported rigid-plastic circular steel plates subjected to localised blast loading. *Int. J. Mech. Sci.* 65(1). p. 177–191.

6. MEHREGANIAN, N., FALLAH, A. S & LOUCA, L. A. (2018) Inelastic dynamic response of square membranes subjected to localised blast loading. *Int. J. Mech. Sci.* 148. p. 578–595.

7. Szilard, R. Theories and applications of plate analysis: classical numerical and engineering methods. – New York: Wiley-Interscience Publication. – 2004.
8. Symonds, P. S. Parkes revisited: On rigid-plastic and elastic-plastic dynamic structural analysis / P. S. Symonds & W. T. Fleming // Int. J. Impact Eng. – 1984. – **2**(1). – P. 1–36.
9. Yuan, Y. Large deformation, damage evolution and failure of ductile structures to pulse-pressure loading / Y. Yuan, P. J. Tan, K. A. Shojaei & P. Wrobel // Int. J. Solids Struct. – 2016. – **96**. – P. 320–339.
10. Zheng, C. The elastic-plastic dynamic response of stiffened plates under confined blast load / C. Zheng, X. S. Kong, W. G. Wu & F. Liu // Int. J. Impact Eng. – 2016. – **95**. – P. 141–153.
11. Rigby, S. E. Elastic-plastic response of plates subjected to cleared blast loads / S. E. Rigby, A. Tyas & T. Bennett // Int. J. Impact Eng. – 2014. –**66**. – P. 37–47.

7. SZILARD, R. (2004) *Theories and applications of plate analysis: classical numerical and engineering methods*. New York: Wiley-Interscience Publication.
8. SYMONDS, P. S. & FLEMING, W. T. (1984) Parkes revisited: On rigid-plastic and elastic-plastic dynamic structural analysis. *Int. J. Impact Eng.* 2(1). p. 1–36.
9. YUAN, Y., TAN, P. J., SHOJAEI, K. A. & WROBEL, P. (2016) Large deformation, damage evolution and failure of ductile structures to pulse-pressure loading. *Int. J. Solids Struct.* 96. p. 320–339.
10. ZHENG, C., KONG, X. S., WU, W. G. & LIU, F. (2016) The elastic-plastic dynamic response of stiffened plates under confined blast load. *Int. J. Impact Eng.* 95. p. 141–153.
11. RIGBY, S. E., TYAS, A. & BENNETT, T. (2014) Elastic-plastic response of plates subjected to cleared blast loads. *Int. J. Impact Eng.* 66. p. 37–47.

Надійшла до редколегії 29.09.19